HYDROCOASTAL

SAR/SARin Radar Altimetry for Coastal Zone and Inland Water Level

River discharge validation
WP3330

Sentinel-3 and Cryosat SAR/SARin Radar Altimetry for Coastal Zone and Inland Water

ESA Contract 4000129872/20/I-DT

Project reference: HYDROCOASTAL_ESA_ _WP3330
Issue: 1.0

This page has been intentionally left blank

Change Record

Date	Issue	Section	Page	Comment
15/06/2023	V1			

Control Document

Process	Name	Date
Written by:	Angelica Tarpanelli, Paolo Filippucci, Stefano Vignudelli and Francesco De Biasio	09/06/2023
Checked by	Angelica Tarpanelli	15/06/2023
Approved by:		

Subject	Radar Altimetry for Coastal Zone and Inland Water Level	Project	HYDROCOASTAL

Author	Organisation	Internal references

	Signature	Date
For HYDROCOASTAL team		
For ESA		

Table of Contents

1. Introduction

1.1. The HYDROCOASTAL Project

The HYDROCOASTAL project is a project funded under the ESA EO Science for Society Programme, and aims to maximise the exploitation of SAR and SARin altimeter measurements in the coastal zone and inland waters, by evaluating and implementing new approaches to process SAR and SARin data from CryoSat-2, and SAR altimeter data from Sentinel-3A and Sentinel-3B.

One of the key objectives is to link together and better understand the interactions processes between river discharge and coastal sea level. Key outputs are global coastal zone and river discharge data sets, and assessments of these products in terms of their scientific impact.

1.2. Scope of this Document

The scope of the document is to present the Hydrocoastal product of river discharge and its quantitative validation with ground measurements for the sites where the in-situ records are available and qualitative evaluation in the drought case study along the Po River occurred in the summer 2022.

1.3. Applicable Documents

AD-01: Sentinel-3 and CryoSat SAR/SARin Radar Altimetry for COASTAL ZONE and INLAND WATER - Statement of Work, V1.0 10/01/2019 Ref: EOP-SD-SOW-2018-089

1.4. Reference Documents

RD-01 HYDROCOASTAL Technical Proposal. V1.1 28/11/2019, SatOC and HYDROCOASTAL team.
RD-02 HYDROCOASTAL Implementation Proposal. V1.1 28/11/2019, SatOC and HYDROCOASTAL team.
RD-03 HYDROCOASTAL Management Proposal. V1.3 26/11/2019, SatOC and HYDROCOASTAL team
RD-04 HYDROCOASTAL Financial Proposal. V1.2 28/11/2019, SatOC and HYDROCOASTAL team
RD-05 HYDROCOASTAL Contractual Proposal. V 1.2 26/11/2019, SatOC and HYDROCOASTAL team

1.5. Document Organisation

The document is organized in the introductory section 1, in the river discharge product presentation and validation described in Section 2. Section 3 describes the qualitative validation of the satellite altimetry product (water level and river discharge) for the extreme events and where Section 4 describes the conclusions.

2. River discharge estimation and validation

The estimation of river discharge by merging altimetry and Near InfraRed sensor data is based on the procedure described in the *D1.3 Algorithm Theoretical Basis Document*.
The equation is the following

$$q = \frac{K}{A_d}\left(\frac{C}{M}\right)^f (H - H_{min})^b \qquad (1)$$

where q is the discharge expresses in $m^3/km^2/day$, H is the water level measured by satellite altimetry, H_{min} is the minimum water level observed by satellite, C/M is the reflectance index given by the Near Infrared images and A_d is the upstream basin area of the gauged station. K, b and f are parameters and they are estimated by the minimization of the Nash-Sutcliffe efficiency, NS, between the simulated discharge and the ground observed discharge. In case the ground records of river discharge are not concurrent with period of analysis with satellite data, the calibration of the three parameters is done by using the discharge modelled by Glofas, available online at the following address: https://open-meteo.com/en/docs/flood-api
The river discharge was calculated for several sites along ten rivers: Po, Mississippi, Rhine, Ob, Ebro, White Nile, Gange-Brahmaputra, Niger. However, Danube and Tiber have been analyzed with the reflectance indices and hence added in this report.
The reflectance index, here called C/M for simplifying the numerous combinations we have for each river, was calculated through three different sensors: MODIS from Aqua and Terra and MSI from Sentinel-2. In the next paragraph the presentation of the reflectance indices and the merging procedure is described, with particular focus on the selected temporal series to be used for the next analysis of river discharge.

2.1. Multispectral images analysis

The multi-temporal analysis of the images in NIR band was carried out on three different products:

- Reflectance from MODIS onboard Terra satellite at 250 m of spatial resolution and nearly daily temporal resolution (MOD09GQ)
- Reflectance from MODIS onboard Aqua satellite at 250 m of spatial resolution and nearly daily temporal resolution (MYD09GQ)
- Reflectance from MSI onboard Sentinel-2 at 20 m of spatial resolution and 5-day of temporal resolution.

As already tested during STREAMRIDE project, each river has its morphological characteristics that make a unique solution difficult to apply. For this reason, along with the original formulation C/M calculated by using two single pixels, a series of combinations, for a total of 36, was applied in order to consider the sediment transport (pixel W), the vegetation (pixel V) and the size of the river in terms of width compared to the size of the image pixel (kernel of 3x3 pixels). For sake of brevity, in the following we reported only the combination with the higher performances in terms of ratio between Pearson correlation and RRMSE (RMSE divided mean of the observed).
Figures 1 and 2 show the plots of the C/M temporal series by MODIS and Sentinel-2 for all the sites analyzed. For each temporal series the outliers are filtered beyond the 2σ and the series are made

dimensionless through their mean and standard deviation. As a result, the signals are quite coincident among the sensors, with some exceptions. Consistency is found between the two MODIS products as expected because the characteristics of the sensors are the same. For the Sentinel-2 some disagreement is found especially for Ebro at Zaragoza, Gange at Baruria Transit and Hardinge Bridge. The reason could be related to the size of the rivers. Indeed, in the case of the Ebro the width ranges around 90 m and could be difficult to get a reliable signal with MODIS data. While for the Gange the reason could be the difficulties in the evaluation of the correct water mask stable in time due to the high dynamics of the river. This could affect the selection of the significant pixels for M (the measurement pixels).

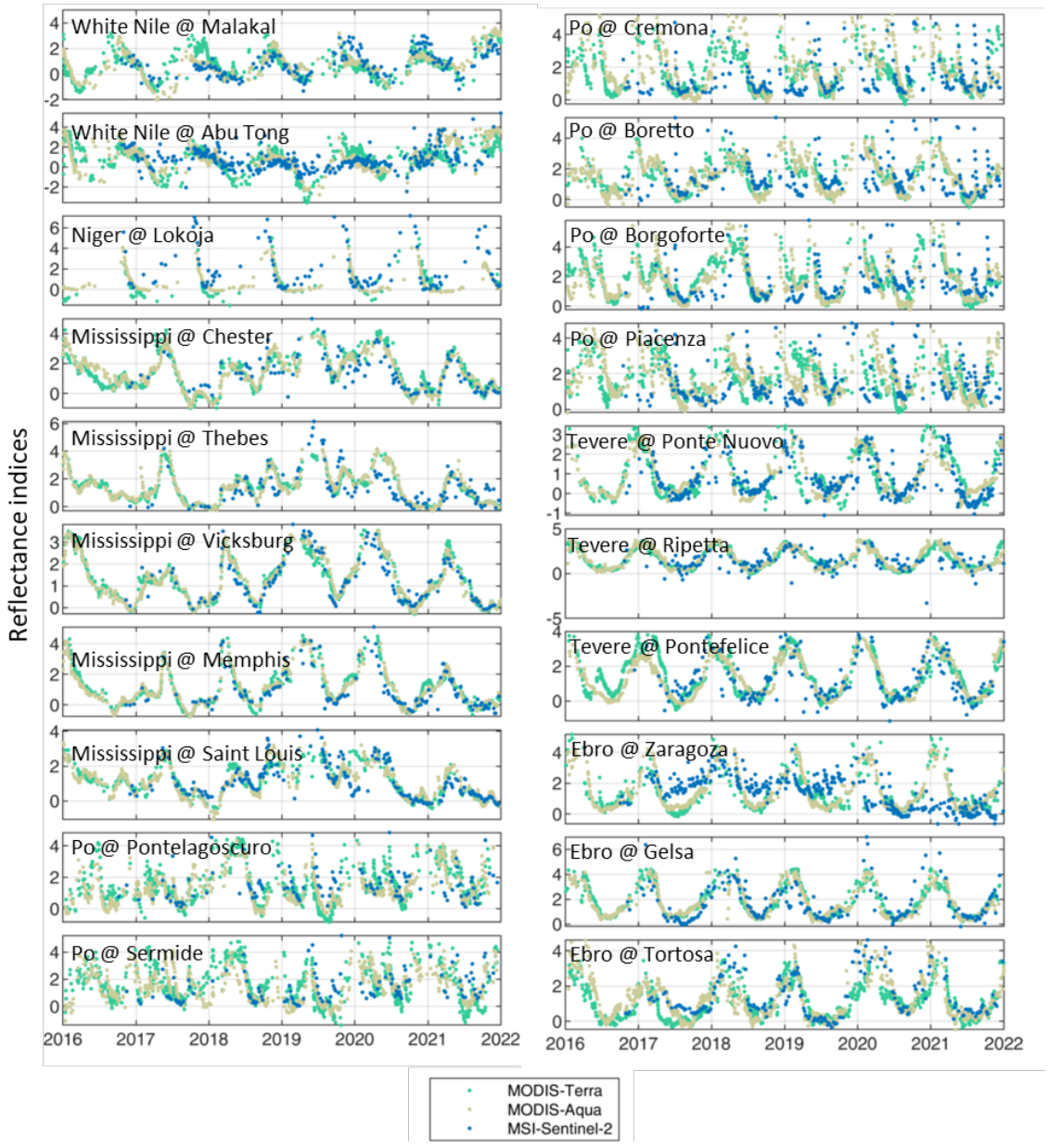

Figure 1: Temporal series of the reflectance indices from three different satellite products (MODIS from Aqua, MODIS from Terra, MSI from Sentinel-2) for twenty sites.

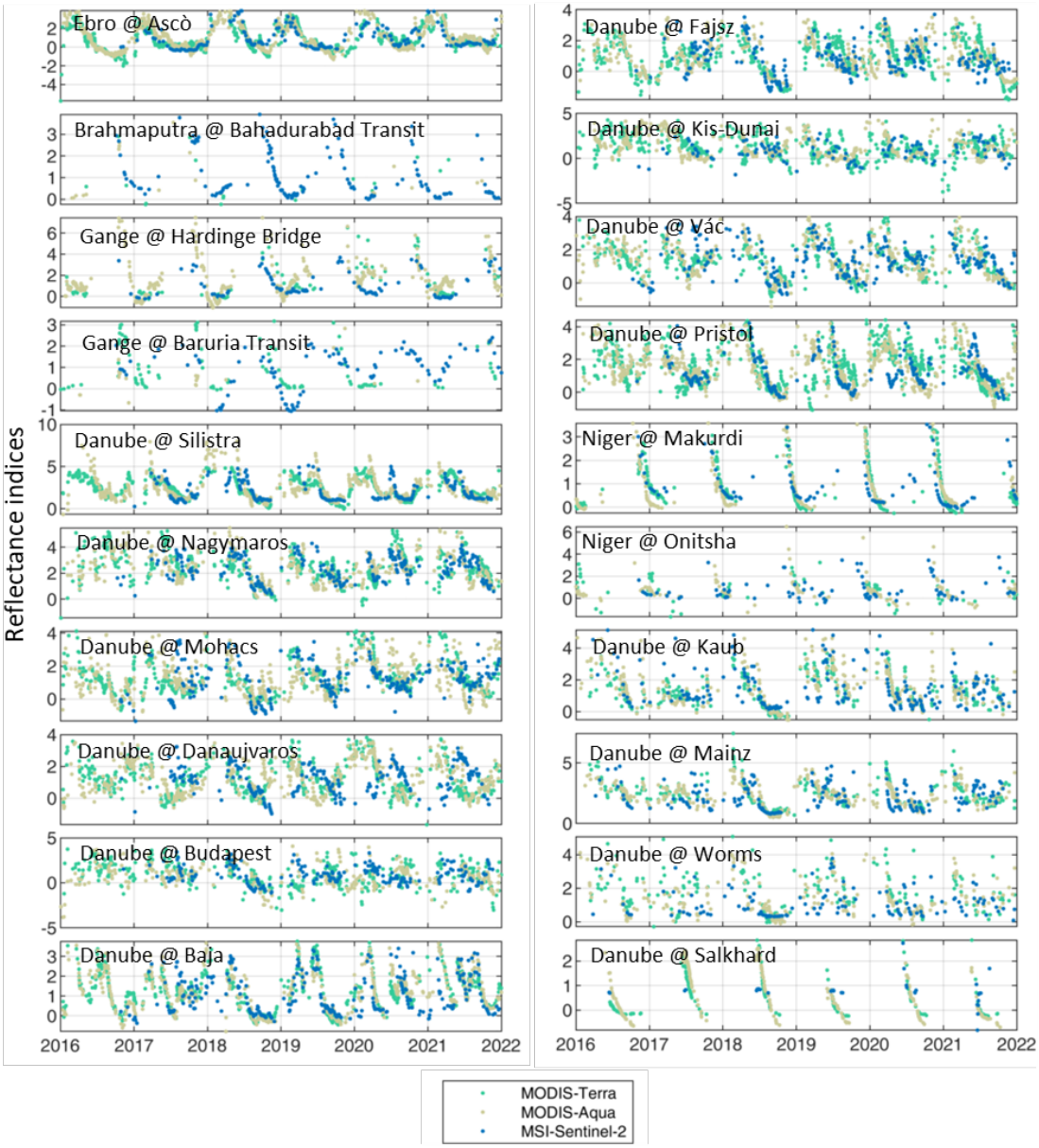

Figure 2: As for Figure 1, but for other twenty sites.

For the merging procedure two approaches were used: the first is described in the paper of Tarpanelli et al. (2020); the second consists in the averaging of the three different reflectance indices and apply a smoothing filter (moving window at 8 days) to the resulting time series. Results of both the techniques are represented in Figure 3 and 4 respectively, compared to the river discharge observed (or modelled) in the sites. The relationship between reflectance indices and river discharge is not unique and the pairs may differ from a fit along the bisector line. However, although they may follow quadratic or exponential laws, the behavior of the former seems more spread than the latter. The correlations calculated confirms this concept as indicated in Table 1. Therefore, the time series derived by the second approach were selected to be used for the combination with the altimetry according the RIDESAT approach.

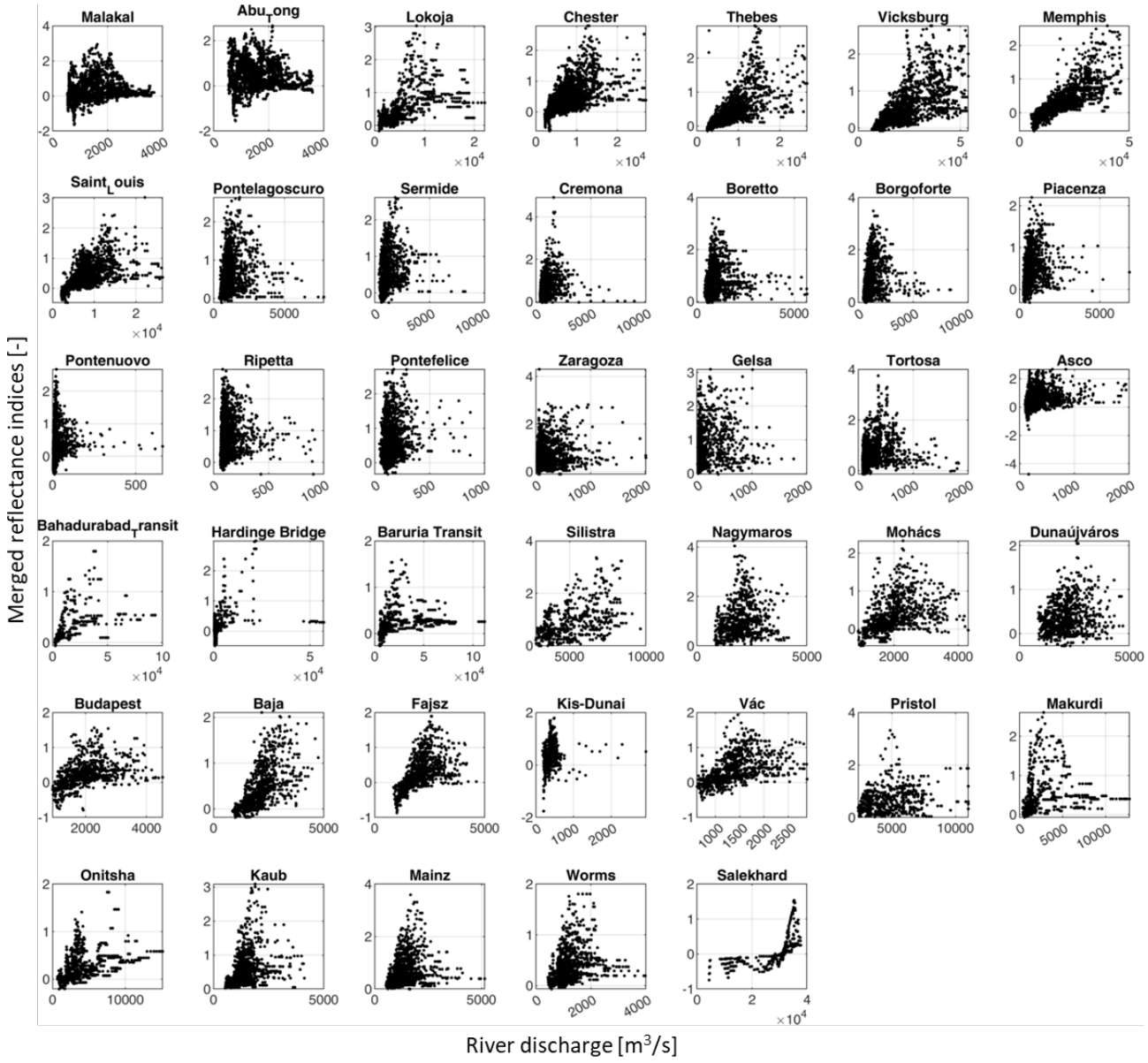

Figure 3: scatterplot of the reflectance indices merged through the paper of Tarpanelli et al. (2020) and the river discharge observed (or modelled) at each site.

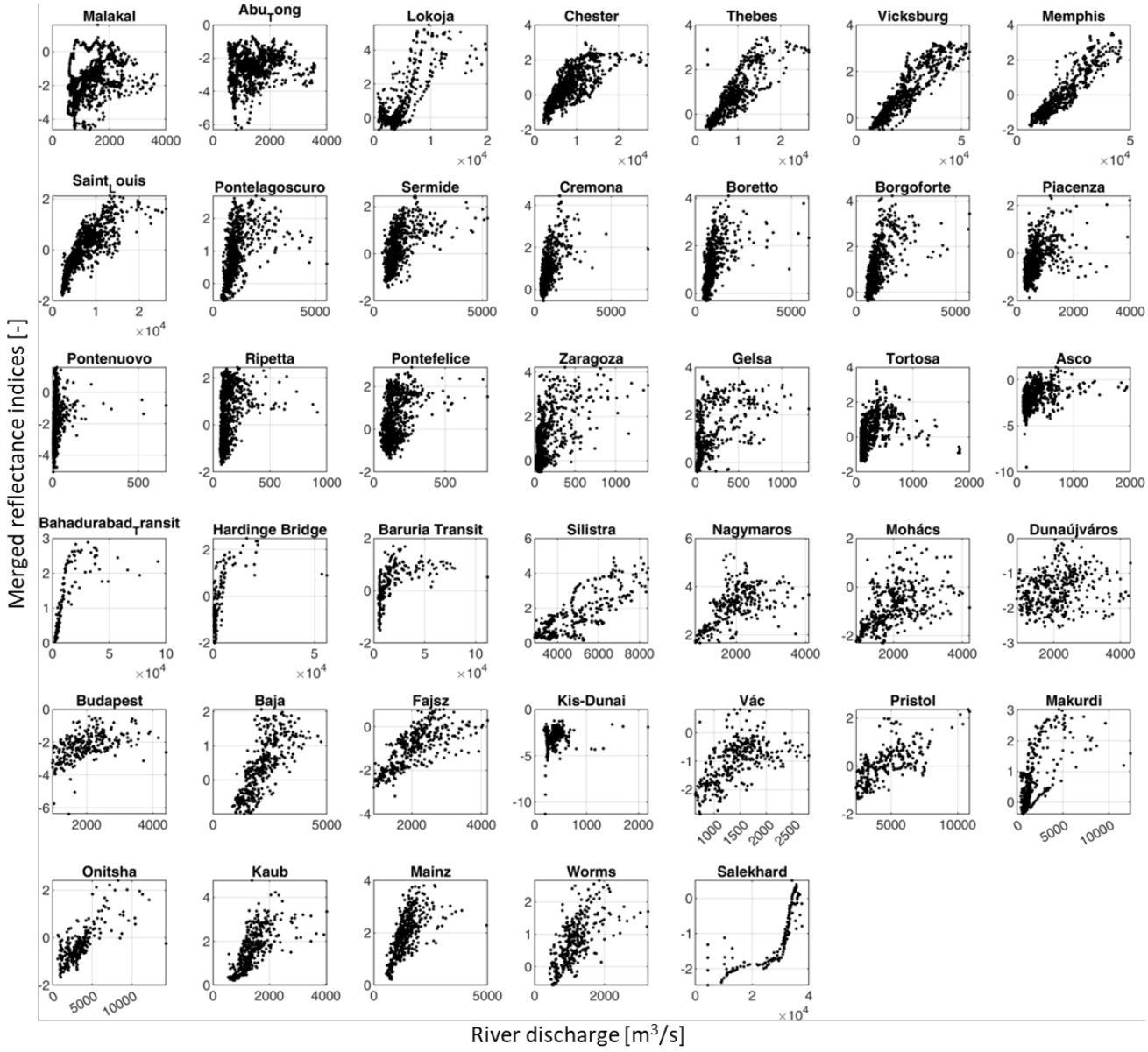

Figure 4: scatterplot of the reflectance indices merged through the average approach and the river discharge observed (or modelled) at each site.

The poor correlation of the first approach is due to the poor matching among the available images. The weights to be assigned to single products are averaged based on a matrix of co-existence of the three products contemporary. If one of the products is missing for a specific date, the weight is not calculated. The co-existence is not obvious among these products especially for the sites located in the tropical areas or arctic regions, where the clouds or ice affect significantly the number of images that can be used in the analysis. Once the weights are calculated (for a few dates) they are averaged and applied to the entire time series of each product. This step implies errors in the final merged time series with a large spread of the reflectance values. Different situation is for the second approach. It includes the single

values of the three products when they are not co-existent, and an average value when two or three products are available the same day. To avoid jump or noisy time series a simple moving window filter is applied every 8 days to smooth the signal. This second solution seems more adequate for the sensors selected in the project and provides good correlations with the observed (or modelled) river discharge as indicated in Table 1.

Table 1: Pearson correlation between the observed river discharge and the merged reflectance indices calculated following two approaches: Tarpanelli et al. (2020) and averaging/filtering the signals

River	*Site*	*Tarpanelli et al. (2020)*	*Average*
White_Nile	Malakal	0.15	0.35
White_Nile	Abu_Tong	-0.02	0.23
Niger	Lokoja	0.62	0.78
Mississippi	Chester	0.58	0.78
Mississippi	Thebes	0.64	0.84
Mississippi	Vicksburg	0.65	0.92
Mississippi	Memphis	0.79	0.92
Mississippi	Saint_Louis	0.62	0.82
Po	Pontelagoscuro	0.14	0.48
Po	Sermide	0.24	0.54
Po	Cremona	0.26	0.62
Po	Boretto	0.12	0.51
Po	Borgoforte	0.26	0.65
Po	Piacenza	0.21	0.48
Tiber	Pontenuovo	0.12	0.24
Tiber	Ripetta	0.13	0.39
Tiber	Pontefelice	0.24	0.47
Ebro	Zaragoza	0.19	0.61
Ebro	Gelsa	0.21	0.61
Ebro	Tortosa	0.29	0.49
Ebro	Asco	0.37	0.50
Brahmaputra	Bahadurabad Transit	0.53	0.69
Ganges	Hardinge Bridge	0.30	0.56
Ganges	Baruria Transit	0.35	0.55
Danube	Silistra	0.49	0.81
Danube	Nagymaros	0.18	0.56
Danube	Mohács	0.39	0.50
Danube	Dunaújváros	0.20	0.20
Danube	Budapest	0.41	0.48
Danube	Baja	0.62	0.75
Danube	Fajsz	0.54	0.73
Danube	Kis-Dunai	0.21	0.21

Danube	Vác	0.48	0.56
Danube	Pristol	0.23	0.66
Niger	Makurdi	0.30	0.67
Niger	Onitsha	0.48	0.73
Rhein	Kaub	0.34	0.69
Rhein	Mainz	0.23	0.64
Rhein	Worms	0.28	0.64
Ob	Salekhard	0.69	0.78

2.2. Altimetric time series

For the time series from altimetry two products were generated. In the first phase of the project the time series of Ob, Rhine, Mississippi and Po have been produced for the period from 2016 (or 2018 in case of Sentinel-3B) to 2020. For the second part of the project time series for the Ebro, Gange and Brahmaputra, White Nile and Niger were produced for the period 2016 – 2022. The Po river were also extended to the entire period for the qualitative validation case study.

Because the ground measurements of river discharge are available for the recent period only for the Ebro, the period of validation was separated by the period of calibration only for the sites along this river and the results are shown in the following.

Single tracks from altimeter missions were considered for the estimation of river discharge, when the conditions of the study area were suitable: no tributaries or disconnections (dam or weir) between the virtual stations and the ground stations. Therefore, more than a time series are produced with the different combination between the altimetry and the reflectance indices. For sake of brevity, only the tracks producing the best performances are reported here.

2.3. L4 River discharge product by merging procedure

2.3.1 River discharge for Po, Mississippi, Rhine and Ob Rivers

Figures 5 - 8 show the temporal series of river discharge obtained from the RIDESAT algorithm compared to the river discharge derived separately by altimetry and reflectance indices through simple rating curve with the ground observations. Generally, the altimetry-derived discharge time series better represent the ground observation with respect to the reflectance indices-derived discharge. However, the number of observations with the NIR images is significantly higher than the altimetry data. The RIDESAT algorithm is able to improve the altimetry performances in the estimation of river discharge as confirmed by the performances reported in Table 2-4. Here, the performances, in terms of comparison between the simulated discharges and the ground observations, defined in the PVP are reported: Mean, Standard Deviation (SD), Pearson correlation (R), Root Mean Square Error (RMSE), Normalized Root Mean

Square Error (NRMSE), Nash-Sutcliffe Efficiency (NSE), Klinge Gupta Efficiency (KGE). In this case the periods of calibration and validation are coincident because it is too short to obtain reliable results.
The use of a single mission, in this case Sentinel-3, does not guarantee a temporal coverage consistent with the multispectral sensors data (nearly daily).

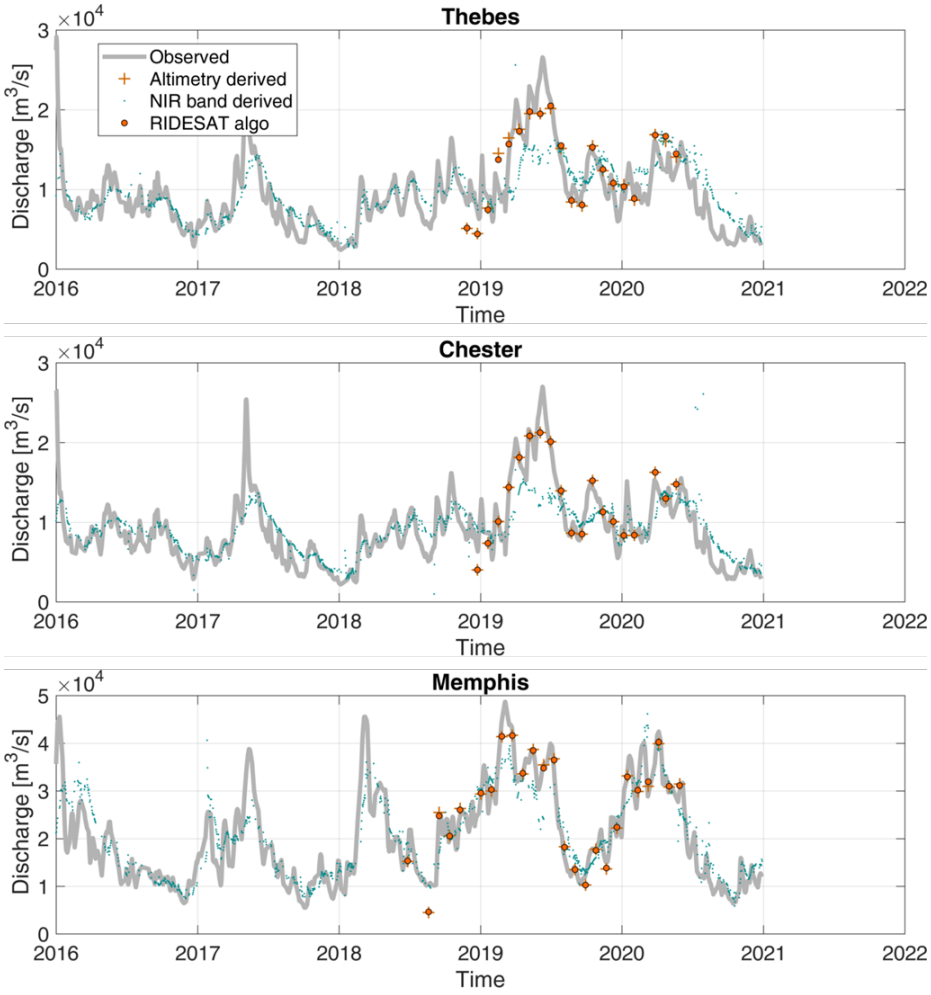

Figure 5: Mississippi River - L4 product of river discharge derived by the merging procedure of the RIDESAT algorithm, along with the river discharge estimated by altimetry and reflectance (NIR band)

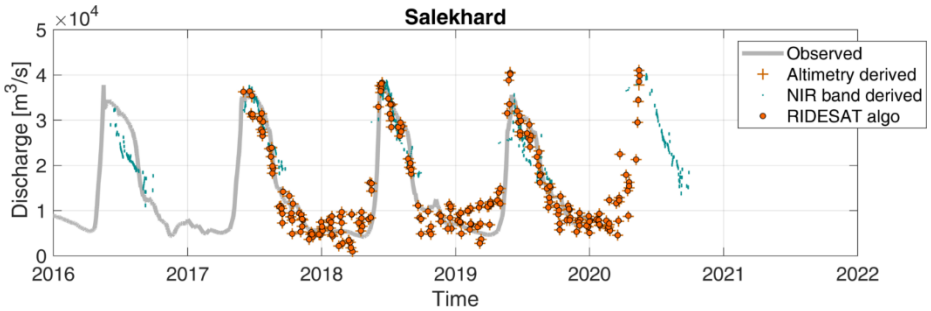

Figure 6: Ob River - L4 product of river discharge derived by the merging procedure of the RIDESAT algorithm, along with the river discharge estimated by altimetry and reflectance (NIR band)

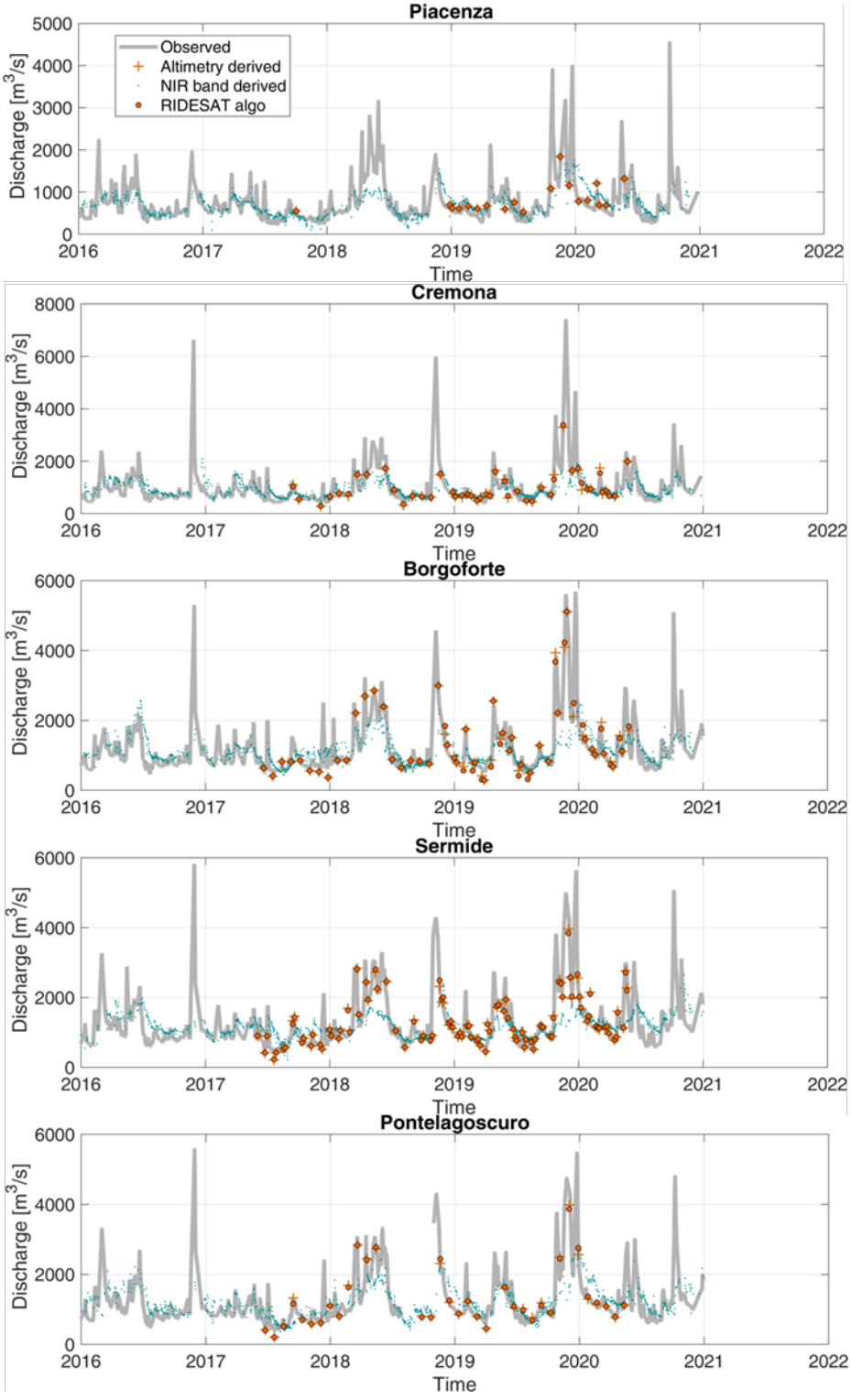

Figure 7: Po River - L4 product of river discharge derived by the merging procedure of the RIDESAT algorithm, along with the river discharge estimated by altimetry and reflectance (NIR band)

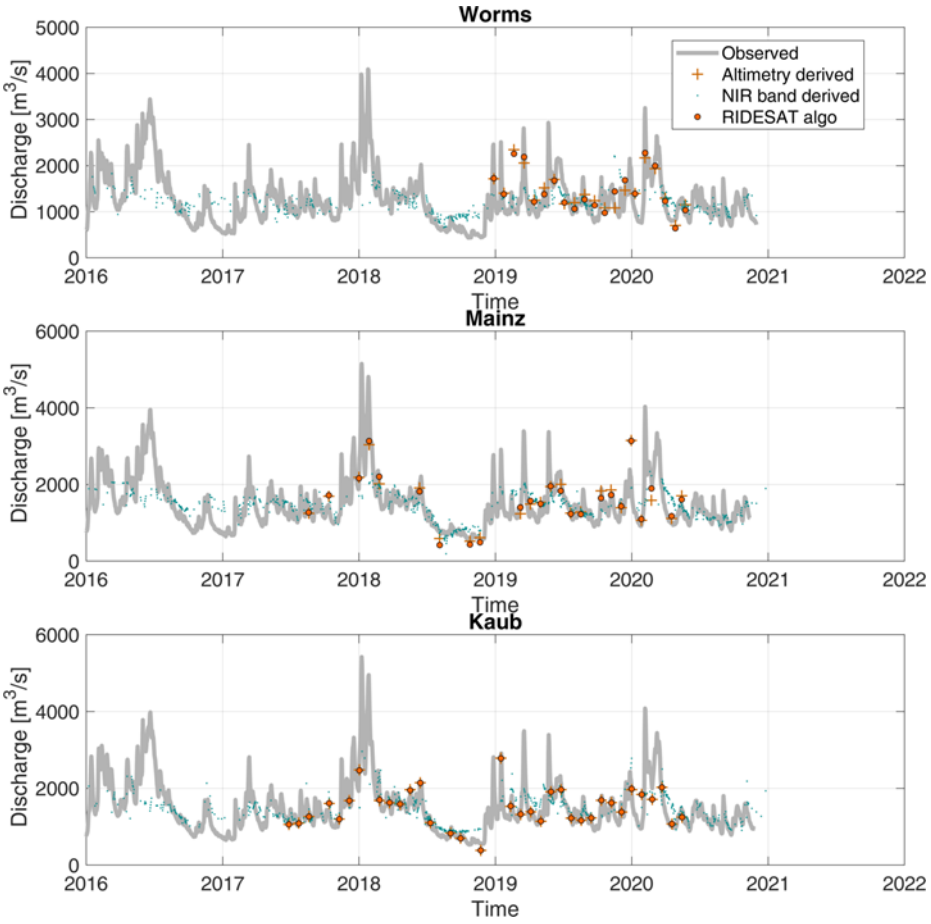

Figure 8: Rhine River - L4 product of river discharge derived by the merging procedure of the RIDESAT algorithm, along with the river discharge estimated by altimetry and reflectance (NIR band)

Table 2: Performances between observed and simulated river discharge obtained by altimetry

	Mean error	*Dev standard error*	*R*	*RMSE/100*	*RRMSE*	*NS*	*KGE*	*mean T*
Piacenza	-4.71	331.38	0.83	3.27	0.40	0.56	0.67	**36.00**
Cremona	9.45	178.11	0.86	1.76	0.18	0.90	0.86	**30.76**
Borgoforte	10.28	283.59	0.95	2.81	0.21	0.92	0.95	**25.36**
Sermide	10.86	307.55	0.89	3.06	0.24	0.84	0.88	**19.58**
Pontelagoscuro	17.30	258.75	0.95	2.57	0.19	0.91	0.95	**20.97**
Thebes	128.83	1447.63	0.98	14.35	0.11	0.92	0.97	**24.50**
Chester	123.49	2740.30	0.82	27.14	0.23	0.70	0.80	**23.47**
Memphis	256.09	3048.57	0.93	30.00	0.10	0.92	0.93	**37.24**
Worms	-9.86	441.15	0.60	4.36	0.31	0.52	0.51	**22.90**
Kaub	-0.54	201.51	0.90	2.00	0.13	0.85	0.90	**20.93**
Mainz	7.25	394.23	0.92	3.90	0.25	0.75	0.84	**29.42**
Salekhard	82.45	4537.81	0.66	45.06	0.31	0.83	0.65	**18.35**
Median	**10.57**	**362.81**	**0.89**	**3.59**	**0.22**	**0.85**	**0.87**	**23.98**
mean	**52.57**	**1180.88**	**0.86**	**11.69**	**0.22**	**0.80**	**0.82**	**25.79**

Table 3: Performances between observed and simulated river discharge obtained by reflectance indices

	Mean error	*Dev standard error*	*R*	*RMSE/100*	*RRMSE*	*NS*	*KGE*	*mean T*
Piacenza	18.95	360.97	0.77	3.61	0.51	0.38	0.53	**1.72**
Cremona	-1.01	458.48	0.75	4.58	0.51	0.30	0.46	**1.73**
Borgoforte	15.66	582.77	0.74	5.83	0.52	0.32	0.48	**1.68**
Sermide	31.26	631.64	0.65	6.32	0.53	0.23	0.33	**1.84**
Pontelagoscuro	24.05	615.20	0.71	6.15	0.49	0.32	0.47	**1.72**
Thebes	91.56	3087.45	0.82	30.87	0.32	0.56	0.69	**2.30**
Chester	124.70	2768.70	0.86	27.70	0.31	0.62	0.75	**2.09**
Memphis	153.27	4887.37	0.91	48.87	0.24	0.77	0.85	**2.19**
Worms	6.89	401.70	0.61	4.01	0.34	0.29	0.36	**3.07**
Kaub	12.06	464.60	0.77	4.64	0.32	0.43	0.54	**2.67**
Mainz	6.27	480.23	0.67	4.80	0.33	0.35	0.46	**2.52**
Salekhard	-691.97	7928.17	0.75	79.45	0.32	0.40	0.56	**5.10**
Median	**17.31**	**598.98**	**0.75**	**5.99**	**0.33**	**0.37**	**0.50**	**2.14**
mean	**-17.36**	**1888.94**	**0.75**	**18.90**	**0.39**	**0.42**	**0.54**	**2.39**

Table 4: Performances between observed and simulated river discharge obtained by RIDESAT algorithm

	Mean error	*Dev standard error*	*R*	*RMSE/100*	*RRMSE*	*NS*	*KGE*	*mean T*
Piacenza	-4.33	331.39	0.83	3.27	0.40	0.56	0.67	**36.00**
Cremona	6.66	164.46	0.89	1.63	0.17	0.92	0.89	**30.76**
Borgoforte	19.54	266.09	0.95	2.65	0.20	0.93	0.95	**25.36**
Sermide	12.43	304.78	0.89	3.03	0.24	0.84	0.88	**19.58**
Pontelagoscuro	21.40	250.52	0.95	2.50	0.19	0.92	0.95	**20.97**
Thebes	127.82	1443.80	0.98	14.31	0.11	0.92	0.97	**24.50**
Chester	105.74	2310.24	0.90	22.88	0.19	0.78	0.88	**23.47**
Memphis	257.57	3050.41	0.93	30.02	0.10	0.92	0.93	**37.24**
Worms	-4.96	420.87	0.59	4.16	0.29	0.56	0.54	**22.90**
Kaub	-0.08	200.89	0.90	1.99	0.13	0.85	0.89	**20.93**
Mainz	14.66	378.65	0.94	3.75	0.24	0.76	0.88	**29.42**
Salekhard	84.76	4537.80	0.66	45.06	0.31	0.83	0.65	**18.35**
Median	**17.10**	**355.02**	**0.90**	**3.51**	**0.19**	**0.85**	**0.88**	**23.98**
mean	**53.43**	**1138.32**	**0.87**	**11.27**	**0.21**	**0.82**	**0.84**	**25.79**

2.3.1 River discharge for Gange, Niger, White Nile, Ebro Rivers

Concerning the rivers analyzed in the second phase of the project, all the analysis were carried out by splitting the period in calibration (01 January 2016 – 31 December 2020) and validation (01 January 2021 – 31 December 2022). Unfortunately, only for the Ebro rivers has data available in this recent period and it was not possible to perform the validation for the rest of the rivers. Indeed, for Gange, Niger and White

Nile, the calibration of the parameters of the RIDESAT algorithm were obtained through the use of modelled discharge by Glofas dataset. Concerning the Ganges - Brahmaputra sites and the Niger sites the cloudy coverage during the monsoon season prevents the observation of the river from the optical sensors. As a consequence, most of the values during the flood events are missing in the RIDESAT algorithm with respect to altimetry-derived discharge.

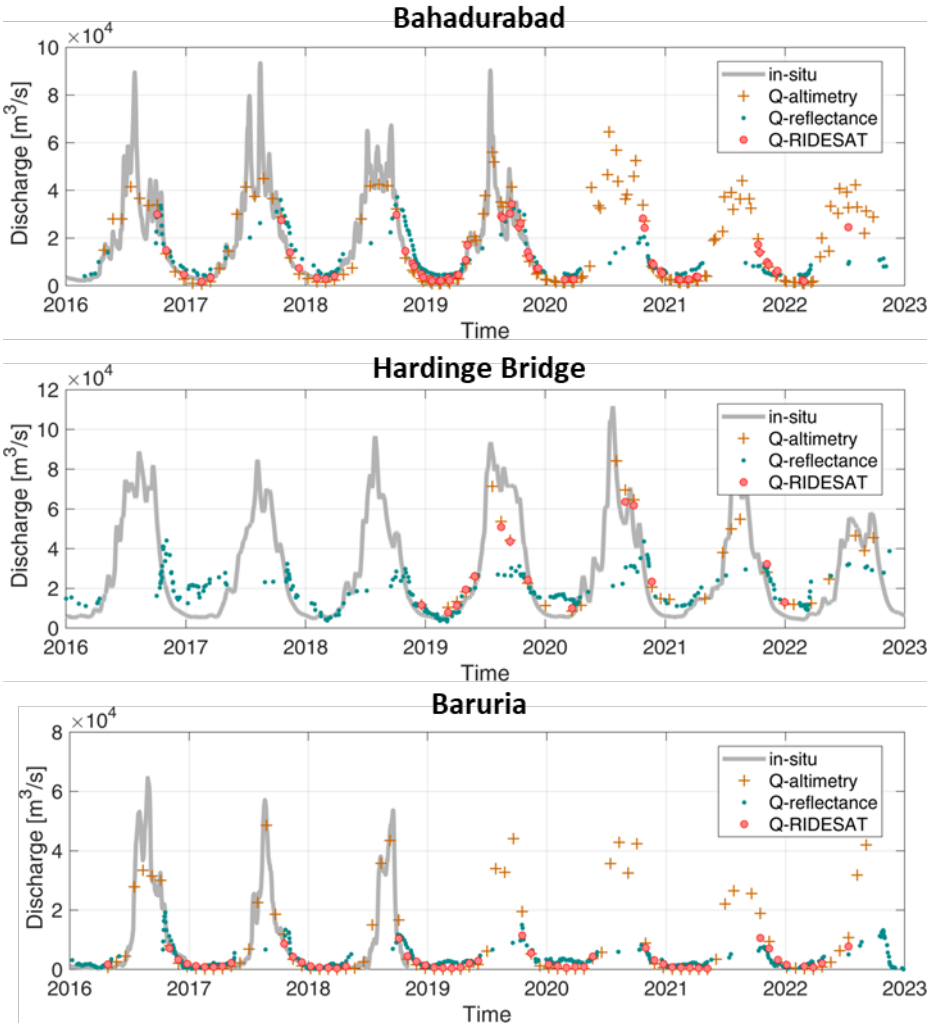

Figure 9: Ganges-Brahmaputra River - L4 product of river discharge derived by the merging procedure of the RIDESAT algorithm, along with the river discharge estimated by altimetry and reflectance (NIR band)

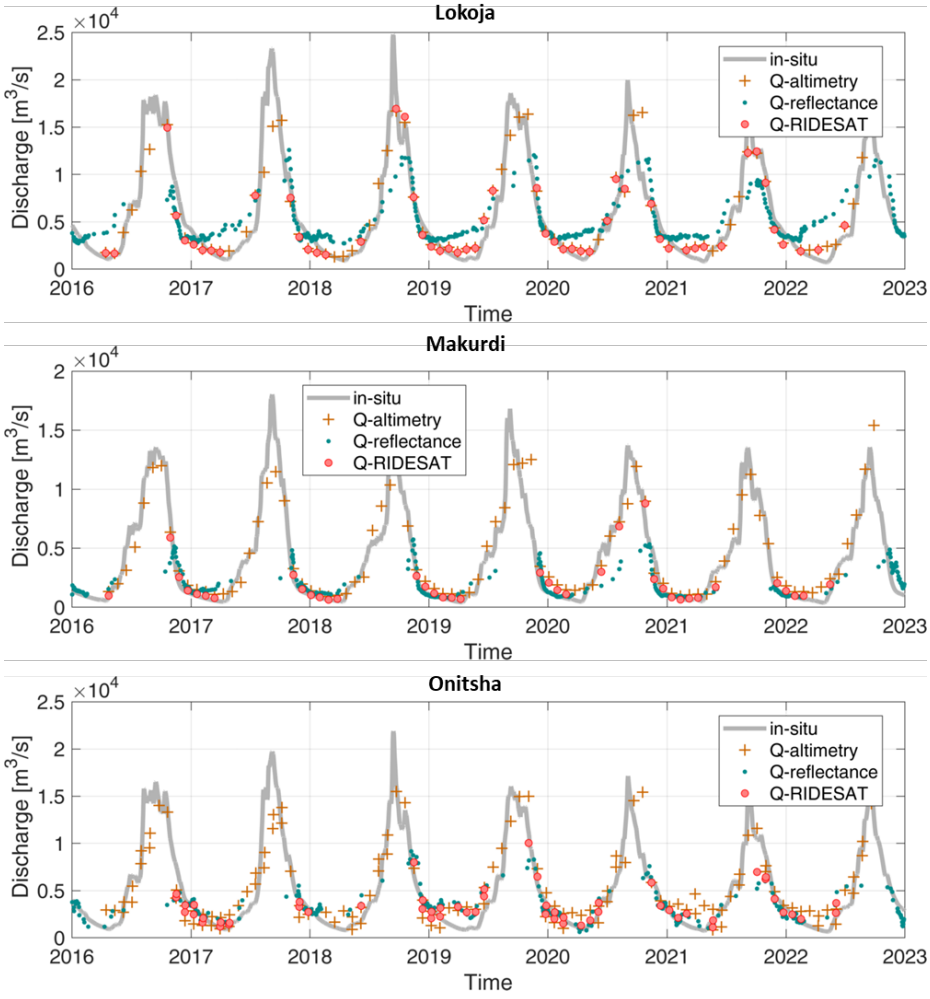

Figure 10: Niger River - L4 product of river discharge derived by the merging procedure of the RIDESAT algorithm, along with the river discharge estimated by altimetry and reflectance (NIR band)

Concerning the Ebro river, the river discharge during the period of validation is available only for the sites of Tortosa and Zaragoza. The performances in calibration and in validation are reported in Table 5 and 6 respectively. As for the previous analysis, the RIDESAT algorithm outperforms the other single mission applications, even if the results are often very similar to the altimetry. In validation the performances decrease especially in Zaragoza where the Relative RMSE reaches an error of the 78%. In this case it is worth to note that the Ebro river is quite narrow and high-resolution satellites are more suitable to analyze this kind of rivers.

In case of White Nile the modelled data extracted by Glofas made not possible to calibrate the parameters of the RIDESAT algorithm, because the large inconsistency with the signal from altimetry and reflectance indices. Therefore, no river discharge is released. However, for sake of completeness, the comparison between the reflectance signal and the water level from altimetry, in terms of anomalies is shown in Figure 12. It is clear that the two sensors are able to see the same characteristics in both the sites with an increasing in the trend from 2021. This is also confirmed by the news about the floods in the areas of the last couple of years. More analyses are needed in the area in order to estimate river discharge.

Table 5: Calibration performances between observed and simulated river discharge obtained by RIDESAT algorithm

	Mean error	*Dev standard error*	*R*	*RMSE/100*	*RRMSE*	*NS*	*KGE*
			TORTOSA				
Altimetry	15.01	129.38	0.59	1.29	0.52	0.65	0.58
Reflectance	-0.97	202.14	0.68	2.02	0.86	0.23	0.37
RIDESAT	17.55	116.44	0.67	1.17	0.47	0.72	0.66
			ZARAGOZA				
Altimetry	4.98	27.50	0.86	0.27	0.17	0.98	0.86
Reflectance	1.18	133.55	0.60	1.33	0.99	0.41	0.46
RIDESAT	4.97	27.51	0.86	0.27	0.17	0.98	0.86

Table 6: Validation performances between observed and simulated river discharge obtained by RIDESAT algorithm

	Mean error	*Dev standard error*	*R*	*RMSE/100*	*RRMSE*	*NS*	*KGE*
			TORTOSA				
Altimetry	32.91	102.30	0.56	1.04	0.44	0.59	0.50
Reflectance	4.01	180.92	0.60	1.80	0.84	0.29	0.31
RIDESAT	42.89	77.84	0.70	0.86	0.37	0.71	0.64
			ZARAGOZA				
Altimetry	-52.54	120.92	0.80	1.28	0.78	0.45	0.28
Reflectance	26.08	133.59	0.53	1.36	1.19	0.22	0.18
RIDESAT	-52.50	120.72	0.80	1.27	0.78	0.46	0.28

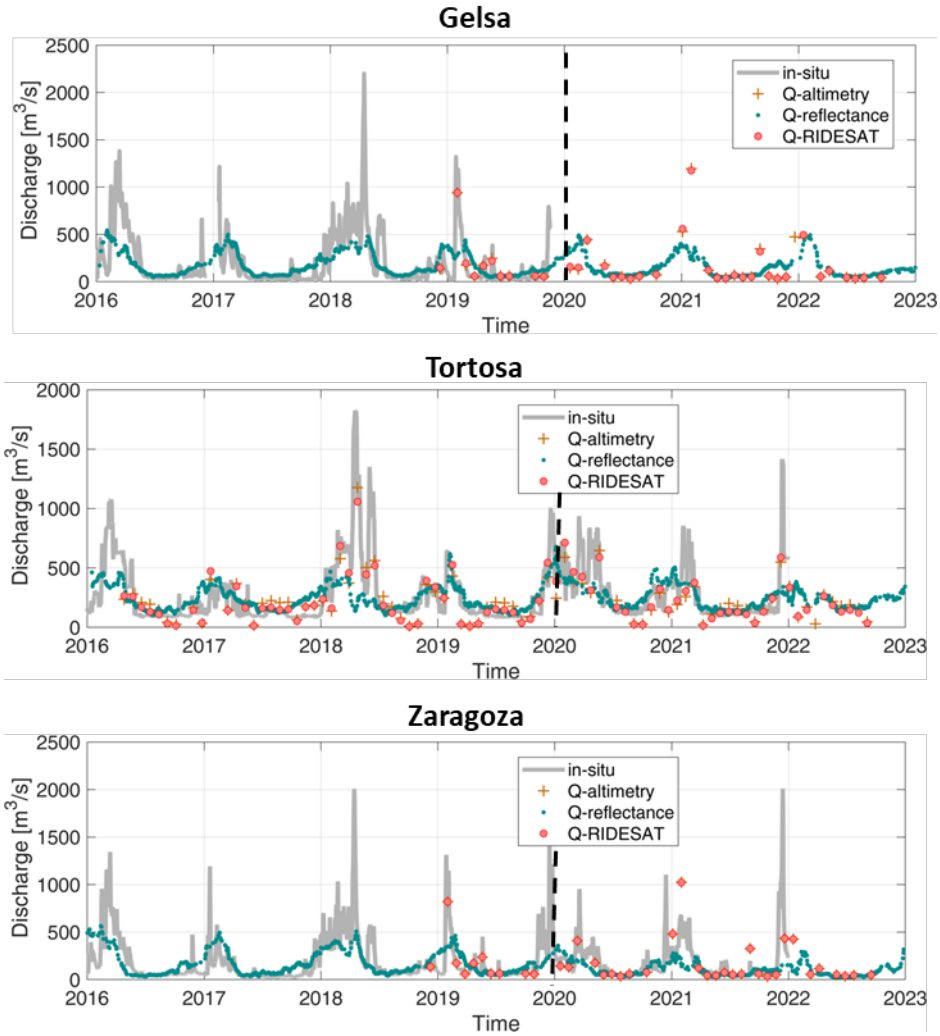

Figure 11: Ebro river - L4 product of river discharge derived by the merging procedure of the RIDESAT algorithm, along with the river discharge estimated by altimetry and reflectance (NIR band). Black dashed line discriminates between calibration (on the left) and validation (on the right) period.

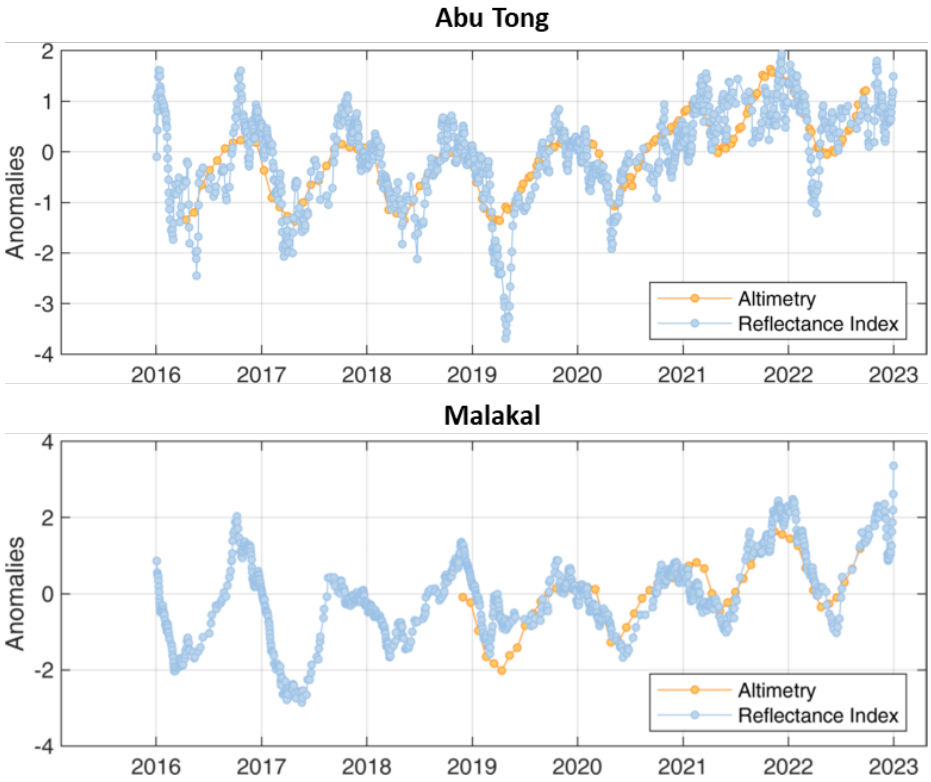

Figure 12: comparison between the water level from altimetry time series and the reflectance indices for the two stations along the White Nile. Both the time series are dimensionless to show the comparison

3. Qualitative validation of the satellite products: case study of the drought event in the Po River

This session describes the qualitative evaluation of the temporal series of water level and river discharge, provided within the Hydrocoastal project. Specifically, the capability to predict extremes events by the L3 and L4 satellite products was tested in the case study of the Po River during the drought event occurred in the summer of 2022.

The Po River is the longest river in Italy with a length of about 660 km. It originates from Pian del Re of Monte Viso, and flows through the Po plain in direction West-East till the Adriatic Sea near Venice. The Po Basin has a drainage area of 71,327 km^2, and hosts a basin population close to 17 million inhabitants (almost 1/3 of the population of Italy). The main land use of the Po basin (about 41 %) is intensive agriculture.

During the summer of 2022, the lack of rainfall and reduced snowfall, together with rising temperatures, caused a drastic reduction in water levels marking this as the worst drought in 70 years for the Po Valley. It had significant impact not only for the agriculture but also for the local residents. Rationalization of drinking water for urban areas and of irrigation of crops in densely populated agricultural areas were just some of the consequences, along with dried-up springs and trampled river beds. The situation was further aggravated by the intrusion of salt water into the river, destroying crops and making irrigation almost impossible (https://www.today.it/attualita/po-fiume-cuneo-salino-siccita-dove.html).

The analysis here carried out aimed to evaluate two aspects: i) if the satellite altimetry was able to monitor the decreasing of the water levels along main water course and ii) if it was possible to observe the intrusion of the salt water in the downstream part of the Po River.

To answer the two questions, several satellite products were collected:

- the L3 product of the Po River related to the Sentinel-3 missions (Hydrocoastal project),
- the L2 product of the Po River related to the Cryosat-2 mission (Hydrocoastal project),
- the L2 product of the plume of the delta related to the Sentinel-3 missions (Hydrocoastal project),
- ATL13 product of Icesat-2 mission of the Po River (https://nsidc.org/data/atl13)
- the water level of the ground stations along the river in the recent period (https://www.agenziapo.it/content/monitoraggio-idrografico-0).

All the products are visible in Figure 13, along with the shapefile of the river.

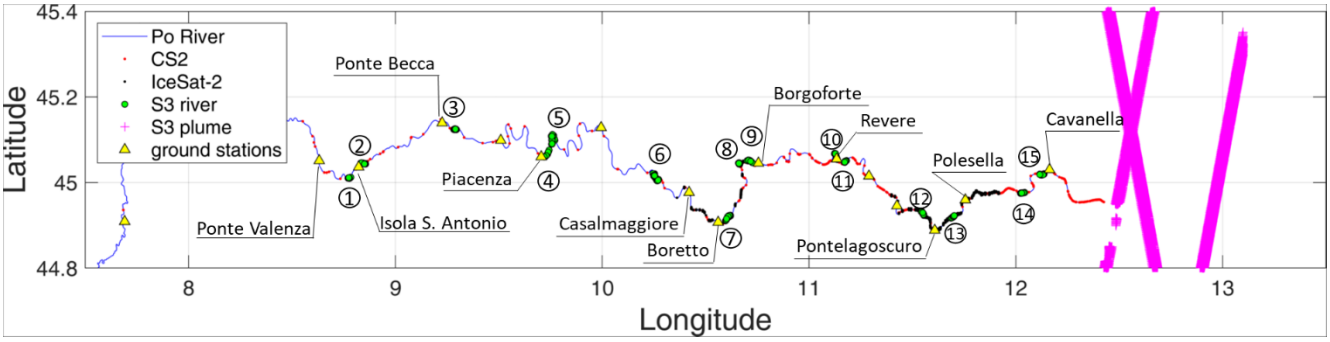

Figure 13: Po River - location of the ground stations and the satellite products (IceSat-2; Cryosat-2: CS2; Sentinel-3: S3)

By looking at the temporal series of the Sentinel-3 product related to the Po River, the effect of the drought in 2022 is evident in almost all the virtual stations released into the project and represented in the plots of Figure 14. Only the first virtual station seems not affected to the decreasing of the water level. This is partially confirmed by the two gauged stations upstream of Ponte Valenza and Isola S. Antonio illustrated in Figure 15, that show only a slight drop in the water level during the summer of 2022 compared to the rest of the year. The situation is different in the middle part of the river with more pronounced lowering of the water surface elevation as in the case of Casalmaggiore or Borgoforte (Figure 15). Comparing the S3 time series the virtual stations close to them (see VS 7, 9 or 10 in Figure 14) similar drops are represented starting from March 2022. The river discharge obtained by the RIDESAT algorithm shows similar trend as shown in detail for the Pontelagoscuro site in Figure 16. Despite the temporal resolution of the altimetry is not optimal for describing the full dynamic of the medium-small rivers, in this case the satellite derived discharge is able to observe a decreasing of the magnitude probably facilitated by the length of the drought event (more than six months).
Looking at the mouth of the river and in particular looking at virtual station 15, the downstream station, the decreasing of the water level is reduced. This effect is probably due to the intrusion of the sea water into the river. In order to analyse this effect, Figure 17 shows the water surface elevation of the different products with the longitude, like a longitudinal profile of the Po river. In particular, only the water level observed in the months of July and August are plotted to show the differences between the year of drought (2022) with the previous years. It is clear the lower value of the Sentinel-3 data in 2022 compared

with the rest of the period, or the other missions (i.e. Cryosat-2) for almost all the longitudinal development. The delta region shows a quite stable levels (tracks 193 and 327) even if compared to the previous year shown lower values: 6.9 cm and 6 cm respectively. Speculating on the results this lowering in 2022 could be due to the missing water coming from the Po river due to the drought event.

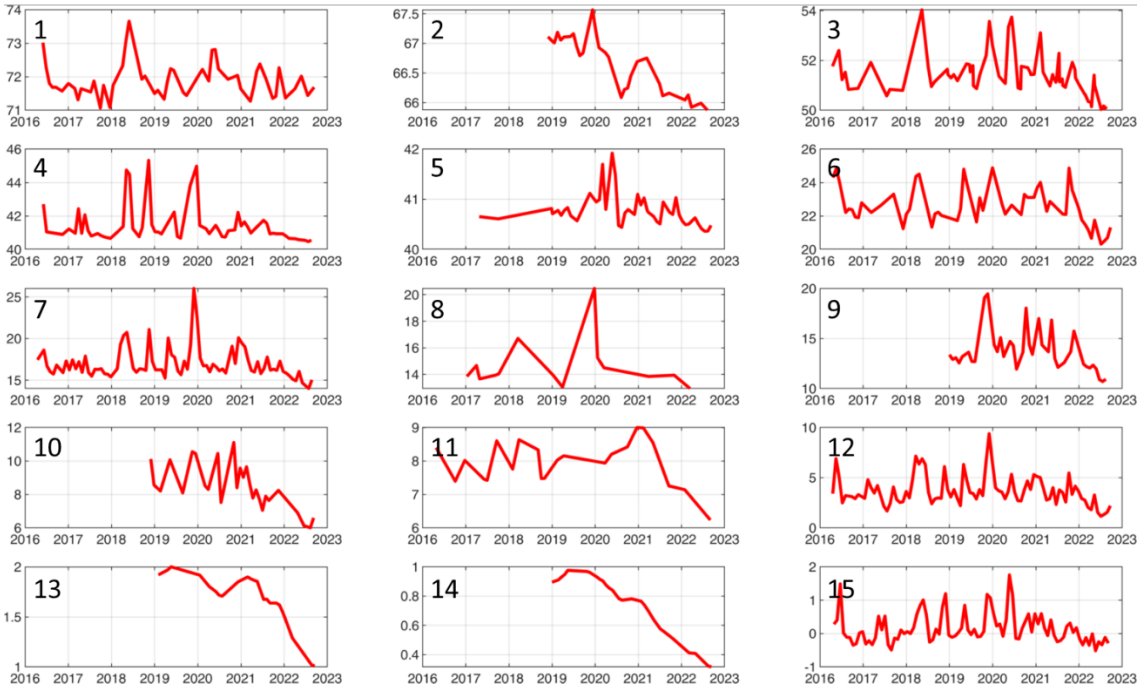

Figure 14: Po River – temporal series of the Sentinel-3 virtual stations from upstream to downstream. For numbers, see Figure 13.

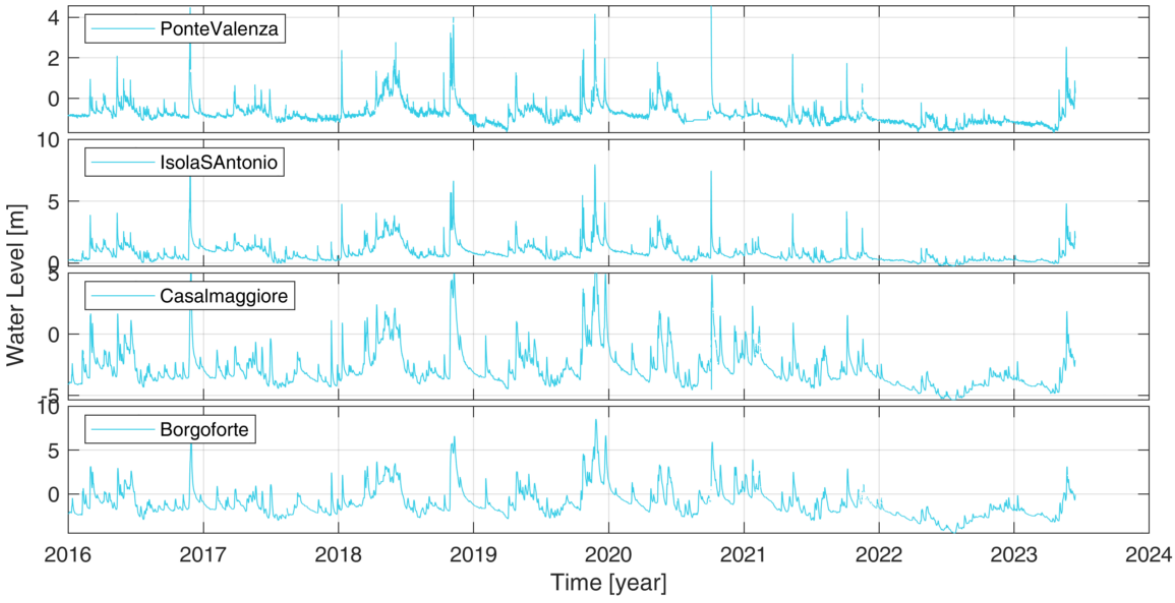

Figure 15: Po River – temporal series of the Gauged stations of Ponte Valenza and Isola S. Antonio Casalmaggiore and Borgoforte (data source: https://www.agenziapo.it/content/monitoraggio-idrografico-0)

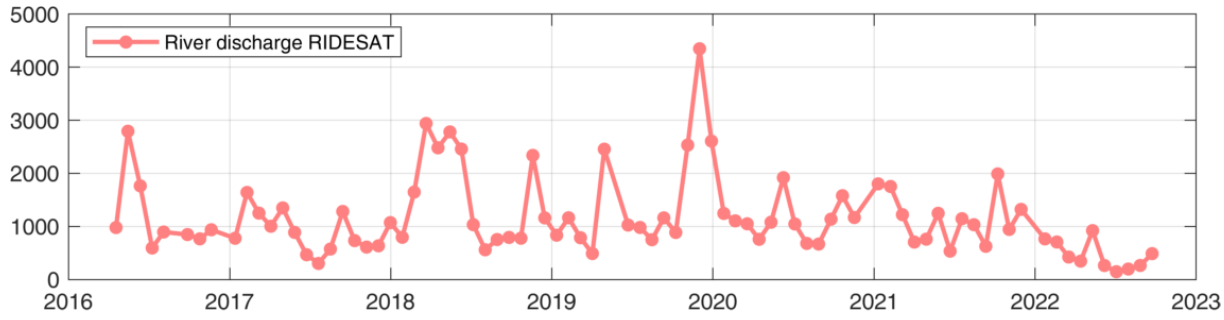

Figure 16: Po River – Temporal series of the river discharge estimated by satellite altimetry and reflectance indices according RIDESAT algorithm for the Pontelagoscuro site.

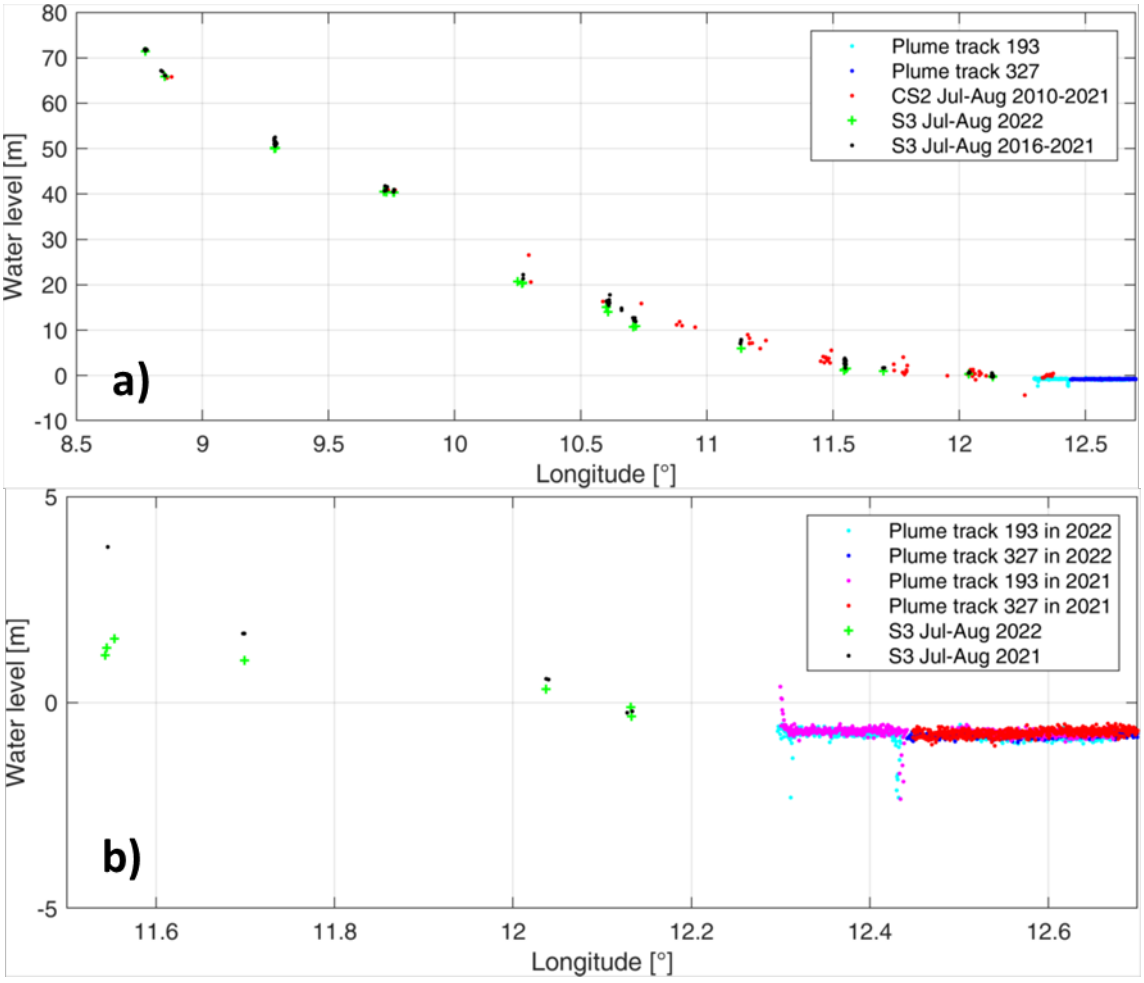

Figure 17: Po River – longitudinal profile of the water levels extracted by the several missions until the delta region (top) and zoom of the delta region (bottom)

Looking in detail on the delta region, Figure 18a illustrates the hydrograph of the water levels of the two gauged stations at downstream of Polesella (about 75 km from the mouth) and Cavanella (about 35 km

from the mouth) from January 2022 to June 2023. While Cavanella shows a large noise due to the tide of the sea level, for Polesella this effect is only visible during the low levels in the summer season, especially in 2022. This effect may be attributed to the intrusion of the salt water not only up to Cavanella as confirmed by the news on the web, but also in Polesella. In order to understand if this effect can be monitored by the satellites, subplots b, c and d of Figure 18 show the Sentinel-3 observations related to the downstream stations 13, 14 and 15 compared to the nearest ground stations measurements extracted at the passage of the satellite. No slope correction is applied in this case, therefore a bias between the satellite and the ground measurements is expected. In terms of general trends, the virtual stations 13 and 14 seems quite constant with a slight decreasing for station 13 from march to the August-September points, confirmed by the Polesella station. For the virtual station 15 the variation is quite significant and can be attributed to the variability of the sea tide as demonstrated by the Cavanella dots.

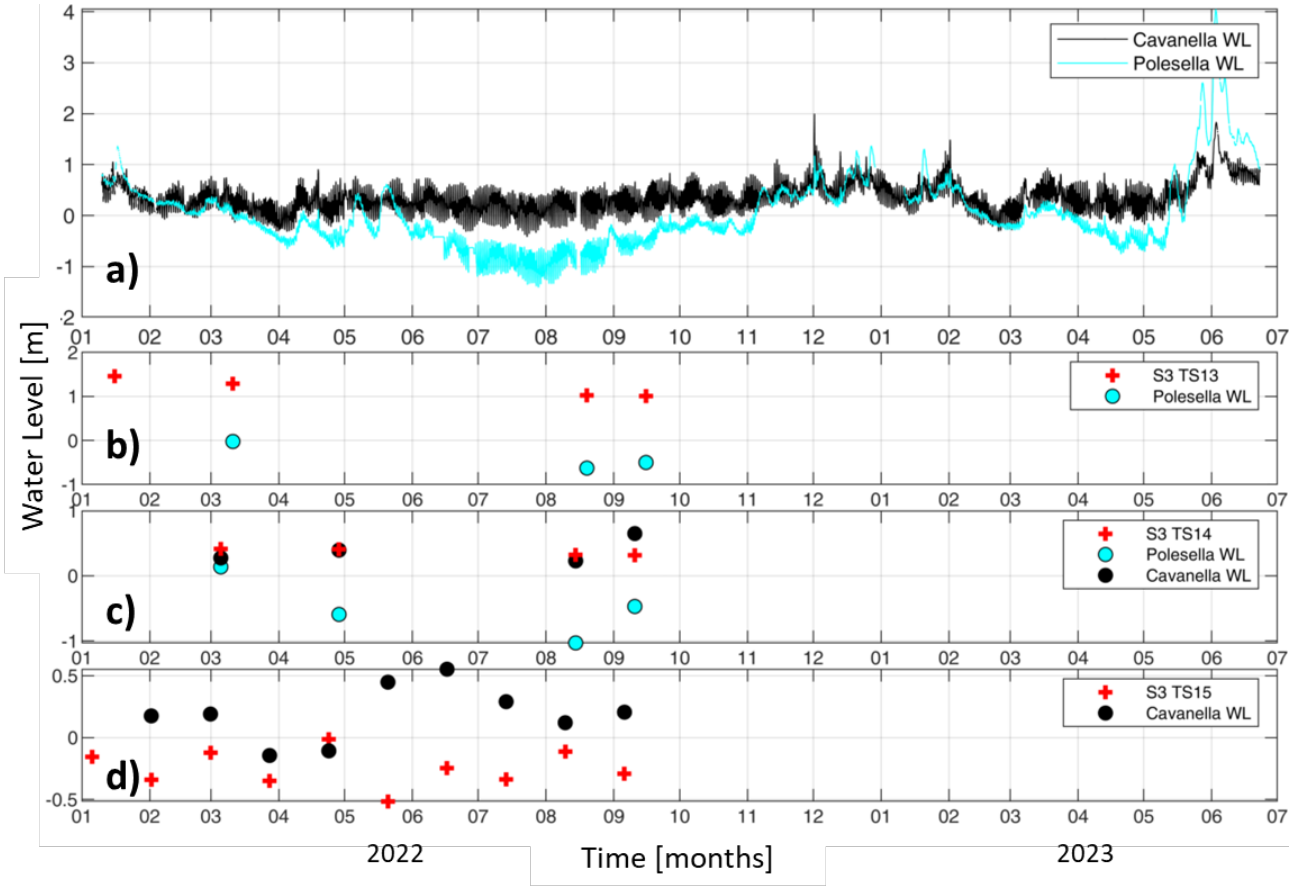

Figure 18: Po River - Temporal series of the two ground stations of Polesella and Cavanella along the Po River (a) and their comparison with the satellite time series at the virtual stations 13 (b), 14 (c) and 15 (d).

4. Conclusions

The report described the product of river discharge and its validation with ground measurements for several rivers across the world. The general evaluation can be summarized in the following points.

- The lack of the multispectral images during the flood periods still remains an open issue especially in the tropical sites or in the arctic sites, where long periods (even months) are completely non-monitored. The ingestion of other multiple optical satellite missions can only partially solve the problem.
- The merging technique of the multi-mission for optical sensors need to be further addressed. A merging technique at the discharge level is probably favourited to avoid jumps or disconnection between the reflectance signals.
- The frequency of the Hydrocoastal products is not suitable to describe the dynamic of the river in almost all the case studies analysed. The use of multi-mission along with merging techniques (Nielsen et al., 2022) is recommended to determine temporal series useful for hydrological applications.
- the river discharge calculated with the RIDESAT algorithm outperformed the other evaluations of river discharge through the independent satellite measurements (e.g. rating curve with the altimetry measurements).

Concerning the case study along the Po River, in order to test the capability of the satellite products of water level and river discharge to detect the extreme events, promising results have been obtained. In particular, all the temporal series of the water level and river discharge show the significant decreasing in the value during the summer 2022. In addition, the analysis of the data at the virtual stations in the downstream part of the Po River along with the data along the tracks of the plume closer to the mouth of the river demonstrated the interaction between sea and river. In particular, the temporal series of the river clearly show the intrusion of the sea for some km along the river (more than 40 km as stated in the news) that caused substantial damages to the agriculture and drinking water aquifers. It is obvious that multi-mission time series with data every 2-3 days is preferable for carrying out the analysis and evaluate in detail the beginning of the drought event and its evolution.

5. References

Nielsen K., Zakharova E., Tarpanelli A., Andersen O.B., Benveniste J. (2022) River levels from multi mission altimetry, a statistical approach. Remote Sensing of Environment, 270, 112876.https://doi.org/10.1016/j.rse.2021.112876

Tarpanelli, A., Iodice, F., Brocca, L., Restano, M., Benveniste, J. (2020): River flow monitoring by Sentinel-3 OLCI and MODIS: comparison and combination, Remote Sensing, *12*(23), 3867, https://doi.org/10.3390/rs12233867